Investigation of Low Temperature Cracking in Asphalt Pavements
National Pooled Fund Study – Phase II

Task 2- Expand Phase I Test Matrix with Additional Field Samples

Subtask on Physical Hardening

Hassan Tabatabaee
Salvatore Mangiafico
Raul Velasquez
Hussain Bahia

University of Wisconsin-Madison

October 2010

TABLE OF CONTENTS

LIST OF FIGURES

List of Tables

Introduction

Physical hardening in asphalt binders was first observed during the Strategic Highway Research Program (SHRP) contract A002-A (1, 2). The phenomenon was called physical hardening by the SHRP researchers (2) to avoid confusion with oxidative aging and to emphasize the reversibility of the phenomenon. It was shown that this phenomenon causes an increase in the asphalt binder stiffness when stored at a constant low temperature. Such isothermal age-hardening has been known for plastics, polymers, and other amorphous solids, but it has been neglected in standard protocols and specification for asphalt binders.

The discovery of physical hardening during the SHRP program resulted in a requirement in the M320 specification (3) of testing in the Bending Beam Rheometer (BBR) after 1 and 24 hours. Although this requirement was not implemented, recent work by Hesp and Subramani (4) has shown that better correlations with field performance are observed if physical hardening is taken into account. One of the main reasons physical hardening has been neglected is the absence of a reliable and simple procedure to estimate the changes in properties (e.g., creep stiffness and m-value) of binders caused by this phenomenon from relatively short and simple laboratory tests.

This report summarizes a comprehensive investigation on the effect of binder source, modification (e.g., Polyphosporic Acid, Warm Mix Additives, etc), glass transition behavior, and thermal history on physical hardening. The asphalt binders studied included materials used in MnROAD sections, the 8-core SHRP binders, and 40 binders from a study conducted by Lu and Isacsson (5).

The details of the development and implementation of a prediction model for physical hardening of asphalt binders is also included in this report. The prediction model was formulated based on a modification of a typical viscoelastic creep model. The model was developed based on experimental data from the 8-core SHRP binders and used to predict physical hardening of MnROAD binders.

Also, this report includes a proposed method to prepare asphalt mixtures samples to be used in measuring dimensional stability of mixtures due to isothermal storage and for glass transition (T_g) temperature testing.

Literature Review

Physical hardening in polymers was first reported by Struik (6). However, the first comprehensive study on physical hardening in asphalt binders was reported during SHRP (1, 2). In asphalt binders as well as many amorphous polymers, physical hardening is a reversible process that occurs at low temperatures. This phenomenon causes time dependent isothermal changes in specific volume and consequently changes in mechanical properties. The effect of physical hardening is completely removed when the material is heated up to room temperatures (2, 6). Physical hardening can be explained by the free volume theory proposed by Struik (6) and Ferry (7).

This phenomenon occurs as a consequence of isothermal reduction of free volume at temperatures close to the glass transition temperature as indicated in Figure 1. The effect of physical hardening is an increase in stiffness and a reduction of the stress relaxation capacity of the asphalt binder.
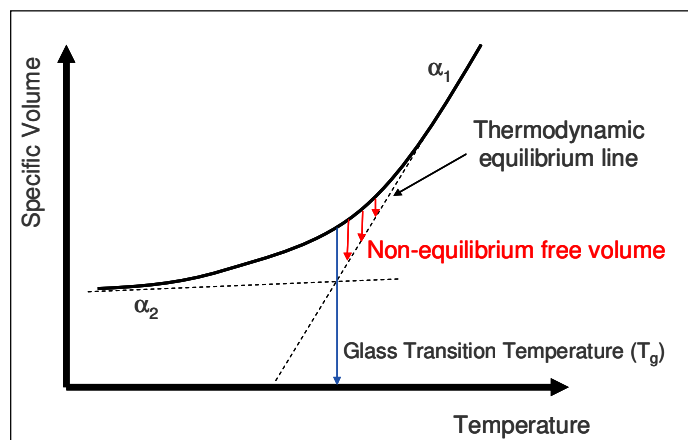
Figure 1: Physical hardening and its relation to free volume

The total volume of the material is constituted by a fraction of occupied volume, which is the volume of molecules and their vibrational motion, and a fraction of free volume due to packing irregularities. Previous studies by Doolittle (8), Doolittle and Doolittle (9), and Williams et al. (10) showed how the internal mobility of amorphous materials is better related to the free volume rather than temperature.

When asphalt binders are cooled down from high temperatures, volume changes due to molecular adjustments are significantly larger than volume changes due to vibrational motion. Therefore, collapse of free volume follows a linear trend with temperature. However, when reaching the glass transition region, the speed of the molecular adjustment becomes slower and the reduction of free volume cannot be accomplished in the experimental time. Thus, further collapse of free volume is due to the reduction of the vibrational motion of molecules. However, if the material is kept in isothermal condition for an extended period of time then the molecular adjustments can take place. These molecular adjustments at isothermal conditions generate significant changes in the free volume and as a consequence changes in the mechanical properties (6). This phenomenon was called physical hardening as reported by Bahia and Anderson (2). Note that in the glass transition region (Figure 1), the asphalt binder is in a meta-stable state (i.e., not in thermodynamic equilibrium) (2, 7) and that first order properties, such as entropy, remain continuous but second order properties, such as coefficients of thermal expansion/contraction and heat capacity, are discontinuous (11).

Bahia and Anderson found that the approach used to account for the effect of changing temperature in viscoelastic materials (i.e., time-temperature superposition principle) can be applied to the stiffening effect of physical hardening with conditioning time by using a shift factor on the time scale. They reported that creep curves obtained at the same temperature but at different conditioning times can be superimposed into a hardening master curve (2). They conducted an extensive study about the relationship between physical hardening and glass transition of asphalt binders and concluded that the concepts used by Struik (6) for amorphous materials can be applied to asphalt binders.

Recent studies have reported that the hardening rate depends on the chemical composition of the asphalt binder (e.g., length of molecular chains and wax content) (12). Moreover, Kriz et al. (13) showed that physical hardening may still occur at temperatures well above T_g due to partial crystallization of some components of the asphalt binder.

Lu and Isacsson (5) investigated the rate of physical hardening for five unmodified and 35 polymer modified binders. They noticed that the hardening index did not always increase with decreasing storage temperature. They also concluded that the kinetics of physical hardening in modified binders seems to be largely dependent on the base binders.

Anderson and Marasteanu (14) showed that physical hardening in asphalt binders occurs both above and below the glass transition temperature, in contrast to amorphous polymers, for which physical hardening occurs only below T_g. The data presented in this paper supported the hypothesis that physical hardening is caused in addition to free volume collapse by the formation of crystalline fractions (1, 15). The authors showed that asphalt binders with higher wax content show stronger physical hardening effects both above and below their T_g.

Romero et al. (16) investigated the effect of different mineral fillers and different volumetric properties on the physical hardening of asphalt mixtures. The authors concluded that fracture rather than strength properties are affected by physical hardening.

Hesp and Subramani (4) investigated low temperature Performance Grade (PG) losses due to reversible aging. They raised the question of whether it is necessary to test in the BBR for 1, 3, and 72 hours, or even longer. The authors observed better correlations with field performance when samples were conditioned for 72 hours. The results from this study indicated that a better measurement of the asphalt binder performance was obtained when physical hardening is considered. Furthermore, the authors showed how physical hardening can affect the reliability of the current method used to classify and select asphalt binders for paving applications.

Materials and Experimental Methods

A total of 55 modified and unmodified asphalt binders were used to investigate the effect of binder source, modification, and thermal history on physical hardening and in the development of the prediction model. A set of 40 binders from a study conducted by Lu and Isacsson (5) were used to develop the concepts behind the model. The results collected for the eight-core SHRP binders were used in the development and verification of the prediction model. Finally, the prediction model was used with physical hardening data obtained from the seven binders proposed in the experimental program of Task 2.

Asphalt Binders

Table 1 shows the materials reference library (MRL) code, PG grade, crude oil source, and glass transition temperature (T_g) of the eight-core SHRP binders. Note that the SHRP binders were aged with the thin film oven (TFO).

Table 2 presents a description of the proposed Task 2 asphalt binders. Note that these binders were subjected to short term aging using the rotating thin film oven (RTFO). Also, a PG 64-22 binder modified with 1% of polyphosphoric acid (PPA) and with 2% of Sasobit®, a warm mix asphalt additive, were tested to assess the effect of these modifiers on physical hardening.

Table 1. SHRP asphalt binders.

MRL Code	PG Grade	Crude Oil Source	T_g (°C)*
AAA-1	PG 58-28	Lloydminster	-28.2
AAB-1	PG-58-22	WY Sour	-13.9
AAC-1	PG 58-16	Redwater	-9.9
AAD-1	PG 58-28	CA Valley	-24.3
AAF-1	PG 64-10	W TX Sour	-6.1
AAG-1	PG 58-10	CA Valley	-9.9
AAM-1	PG 64-16	WTX Inter	-4.1

*From Bahia (2)

Table 2. Asphalt binders selected for Task 2.

Binder	Location	Description
PG58-34 PPA	MnROAD 33	Modified with Polyphosphoric Acid (PPA)
PG58-34 SBS+Acid	MnROAD 34	Modified with Styrene-Butadiene Styrene (SBS) +PPA
PG58-34 SBS	MnROAD 77	Modified with SBS
PG58-34 Elvaloy +Acid	MnROAD 77	Modified with PPA + Elvaloy
PG58-28	MnROAD 20	Neat
PG58-34	MnROAD 22	Neat
Wisconsin	Wisconsin	Binder used in construction of SMA pavement
PG 64-22 – New York	New York	Typical binder used in New York

Test Methods

The measurements of physical hardening were obtained by measuring the change in creep stiffness (S) of asphalt binder beams with isothermal age at different temperatures. All measurements were collected using the Bending Beam Rheometer (BBR) and following AASHTO T 313-05 (17). The asphalt binder beams from the MnROAD cells (Table 2) were tested after 1, 4, 24 and 72 hours of isothermal conditioning time at -12, -18 and -24°C. The SHRP binders were tested after 2, 6, 24 and 96 hours at -10, -15, -25 and -35°C and the binders studied by Lu and Isacsson (5) were tested at 1, 4 and 24 hours at -15, -25 and -35°C.

The glass transition temperature (T_g) of the asphalt binders in Table 2 was measured with a dilatometric system developed at the University of Wisconsin-Madison. Note that no standard for this equipment is available and therefore the test was performed following procedure developed by Bahia and Anderson (18) and later modified by Nam and Bahia (19). The concept behind the procedure is based on precise measurements of volume change in time of an asphalt binder specimen when the temperature decreases at a constant rate. For T_g test, the sample is

prepared by pouring 10 g of hot asphalt into a circular silicone rubber mold with a diameter of 40 mm and a height of 8.0 mm.

The dilatometric cell is connected to a vertical capillary tube (i.e., $\phi = 1$ mm) with its top end open. The volume changes in the sample are calculated by estimating the change in the height of the ethyl alcohol column inside the capillary tube. For this study, the system was further modified by using very precise pressure transducers (Figure 2) to measure the changes in alcohol column height.

Calculation of the glass transition temperature (Tg) is based on a non-linear model proposed originally by Bahia (2) and later successfully used by Nam and Bahia (19). Figures 2 and 3 shows the dilatometric system and typical results for T_g measurements, respectively.
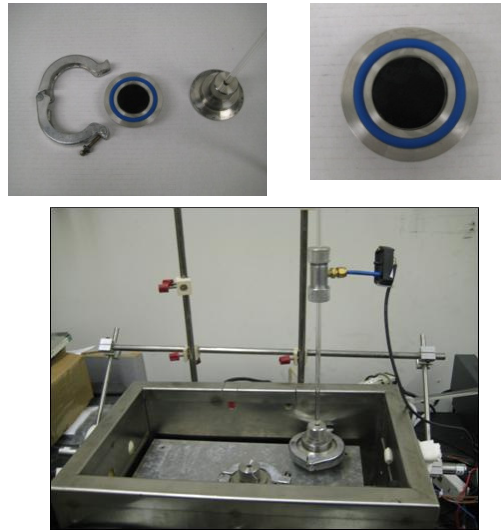
Figure 2: Dilatometric system used to measure glass transition temperature (T_g) of asphalt binders.
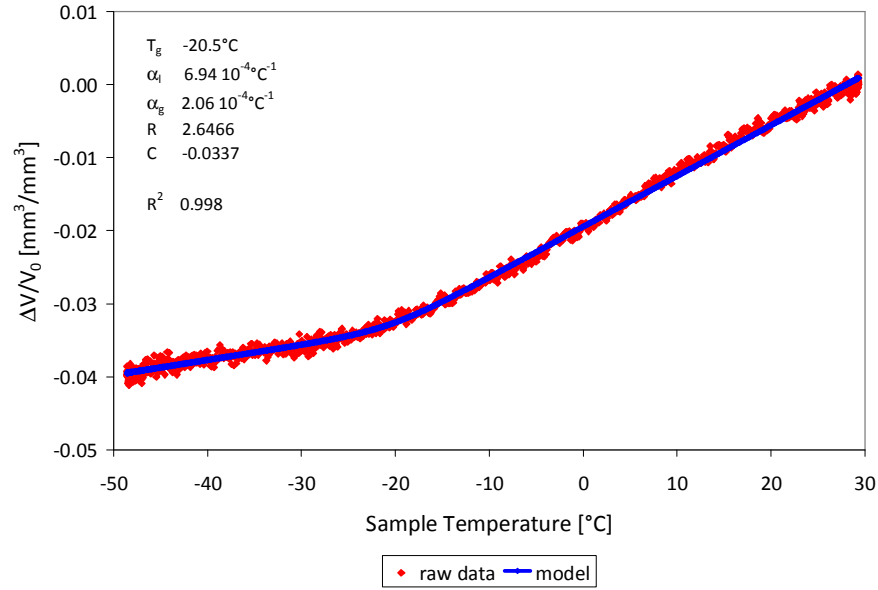
Figure 3: Typical results from glass transition temperature (T_g) test of asphalt binders.

To investigate the effects of thermal history on physical hardening, the asphalt binders in Table 2 were subjected to a thermal cycle consisting of successive isothermal conditioning periods at different temperatures as shown in Figure 4. The thermal cycle included a cooling and heating phase. The selected conditioning times and temperatures were 1, 4 and 24 hours, and -12°C, -18°C and -24°C, respectively. Creep tests were performed during the cycle to measure low temperature rheological properties.
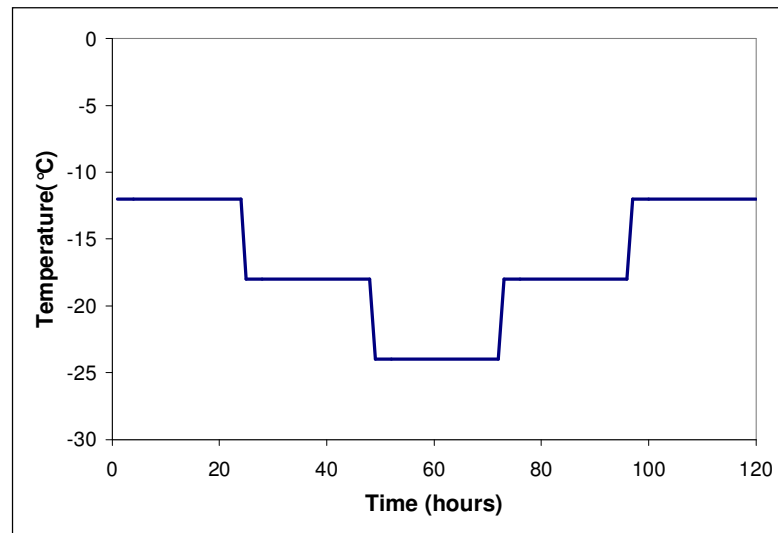
Figure 4: Thermal cycle.

Results and Discussion

Effect of Binder Source and Modification

A hardening index, S_i/S_0, defined as the ratio of the creep stiffness, S(60), after time t_i of isothermal storage to the initial stiffness measurement after time t_0 of isothermal storage (t_0 is always equal to one hour in this report), is generally used to show the rate at which physical hardening occurs at different isothermal conditions (5, 13, and 20).

Although generally assumed that at lower isothermal condition temperatures the rate of physical hardening increases, some studies suggest otherwise. Figure 5 shows that for all SHRP binders, the hardening rate at -35°C was in fact less than the rate at -25°C. Lu and Isacsson (5) tested a wide array of modified and unmodified binders and observed that although for three of the five tested base binders the maximum hardening index was achieved at the lowest experimental temperature (i.e., -35°C), for the other two base binders and their corresponding modified binders, the maximum rate was observed at higher temperatures (5).

These observations indicate that the concept of ever increasing hardening rates as the temperature decreases is not valid as a general rule and that a lower temperature limit to physical hardening occurrence may exist.
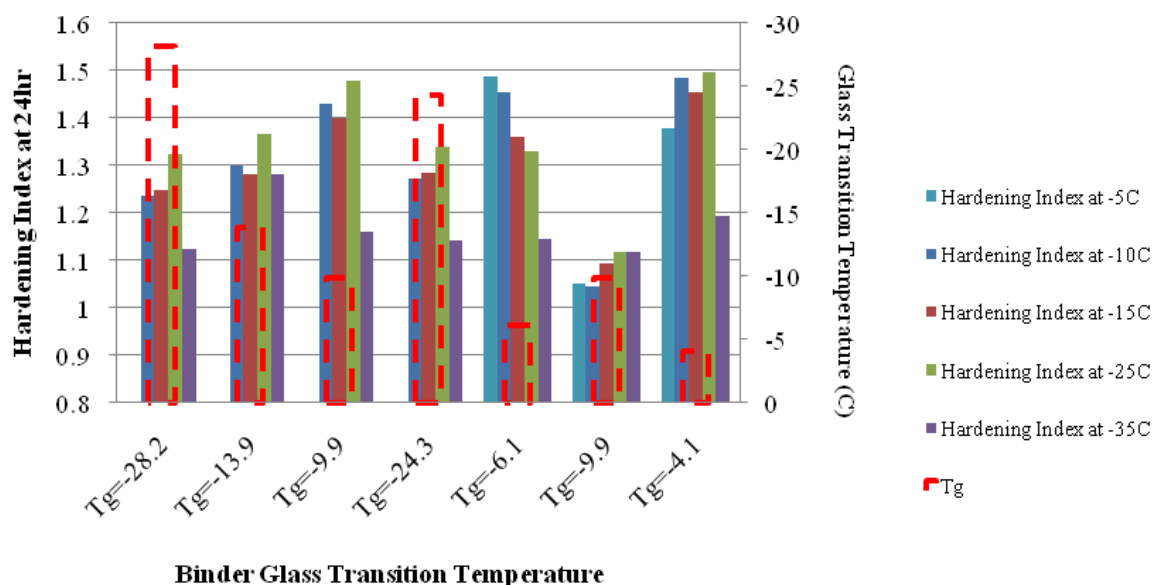

Figure 5: Hardening index after 24 hr (relative to one hour) of isothermal conditioning at different temperatures for SHRP binders.

Figure 6 shows the hardening index and glass transition temperature from tests conducted by Lu and Isacsson (5). As it was observed with the SHRP binders, the rate of hardening at -35°C is less than the rate at -25°C for many of the binders.
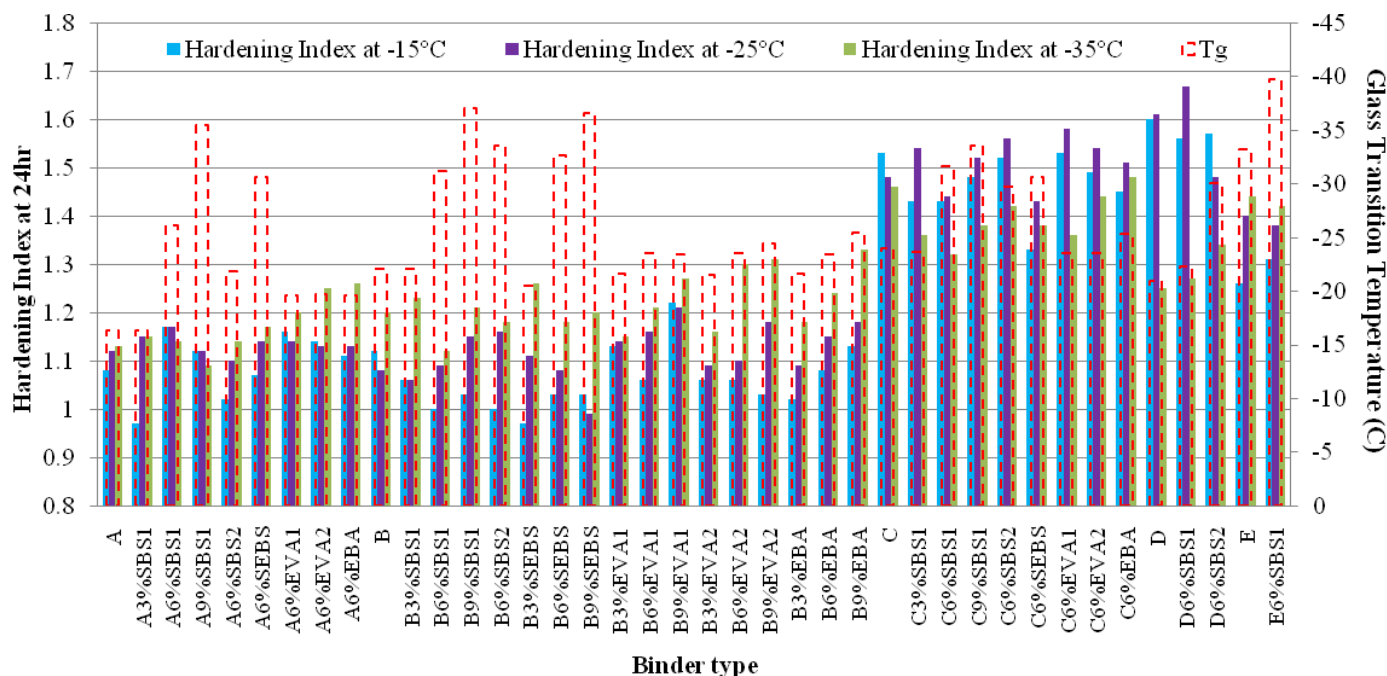
Figure 6: Hardening index after 24 hr of isothermal conditioning at different temperatures using data from Lu and Isacsson (5).

To investigate the effect of modification on the rate of physical hardening, the data collected by Lu and Isacsson (5) was used to conduct ANOVA test at 95% significance level. Three of the base binders modified with five types of modifiers (i.e., three elastomers and two plastomers at a 6% concentration) were selected for this analysis. The results showed that the base binder source is a very significant factor, while polymer modification is insignificant. Furthermore, it was observed that the temperature corresponding to the maximum hardening rate is more or less constant for all modifications of each base binder.

A similar analysis was done on the actual hardening index at -25°C and using the maximum hardening index at the three testing temperatures. The ANOVA results for both cases showed that the base binder is very significant in the prediction of hardening rate, while the type of modification was insignificant at a 95% significance level.

The results analyzed indicate that the base binder properties are the controlling factor for the rate of hardening and that the physical hardening behavior of the base binder phase will dominate the modified binder's hardening rate.

Physical Hardening and Glass Transition

According to the free volume concept as described by Struik (6), as the amorphous material is cooled, the molecular transport mobility, M, and the molecular free volume, v_f, decrease simultaneously. Since molecules attract each other and free volume consists of voids within the molecules, the existence of free volume represents an increase in internal energy, ΔU, with respect to the zero-free volume state. The existence of free volume is accompanied by an increase in entropy, ΔS. Thus, the increase in internal energy due to free volume, ΔU, must be balanced with $T\Delta S$, where T is temperature. The rate of this process is determined by the

segmental mobility, M, which itself is a function of the free volume, v_f. This implies a non-linear trend to the volume relaxation phenomena (6).

The free volume cannot decrease indefinitely as temperature decreases, and at a certain temperature, M becomes so small that the decrease in v_f becomes insignificant. This temperature is referred to as the glass transition temperature, T_g. The small values of M at temperatures below T_g indicates that the volume continues to decrease very slowly over time. The reduction in mobility M in temperatures close to T_g will significantly affect the rate in which the free volume collapses to the equilibrium state (6).

Although many researchers agree upon the effects of physical hardening, there is some disagreement about the temperature range in which physical hardening occurs (*14*). Generally, it is claimed that physical hardening occurs below the glass transition temperature (5, *6*). Experimental data in this study shows that the occurrence of physical hardening begins well before reaching the glass transition temperature.

Glass transition temperature is determined as the temperature at which the two asymptotes to the linear regions before and after the glass transition on the volume-temperature curve intersect. However, the glassy transition begins well before this point (i.e., where the material starts to deviate from thermodynamic equilibrium), thus according to the free volume concept physical hardening will occur as the material enters this transition region.

The existance of a "peak" in the hardening rate as the temperature is decreased, and the subsequent decrease in the rate of hardening observed in the experimental data as temperature falls bellow the peak temperature in many of the tested binders, suggests the existence of a lower temperature limit to the occurrence of physical hardening. This is schematically shown in Figure 7.

The decrease in rate implies that there is a limiting temperature for which the material no longer tends toward the original equilibrium line, but toward a state with a higher energy level than the thermodynamic equilibrium state, shown with the red arrows in Figure 7. This is hypothesized to be the extension of the linear region occurring below the glass transition region. Thus, as the temperature is further decreased, the rate of physical hardening will continue to decrease, ultimately reaching a negligible level at the end of the glass transition region.

Figure 7 and the experimental results indicate the potential importance of the glass transition region in the occurrence of physical hardening, suggesting that any accurate prediction model for physical hardening should include the position of the target temperature relative to the glass transition region of the binder.
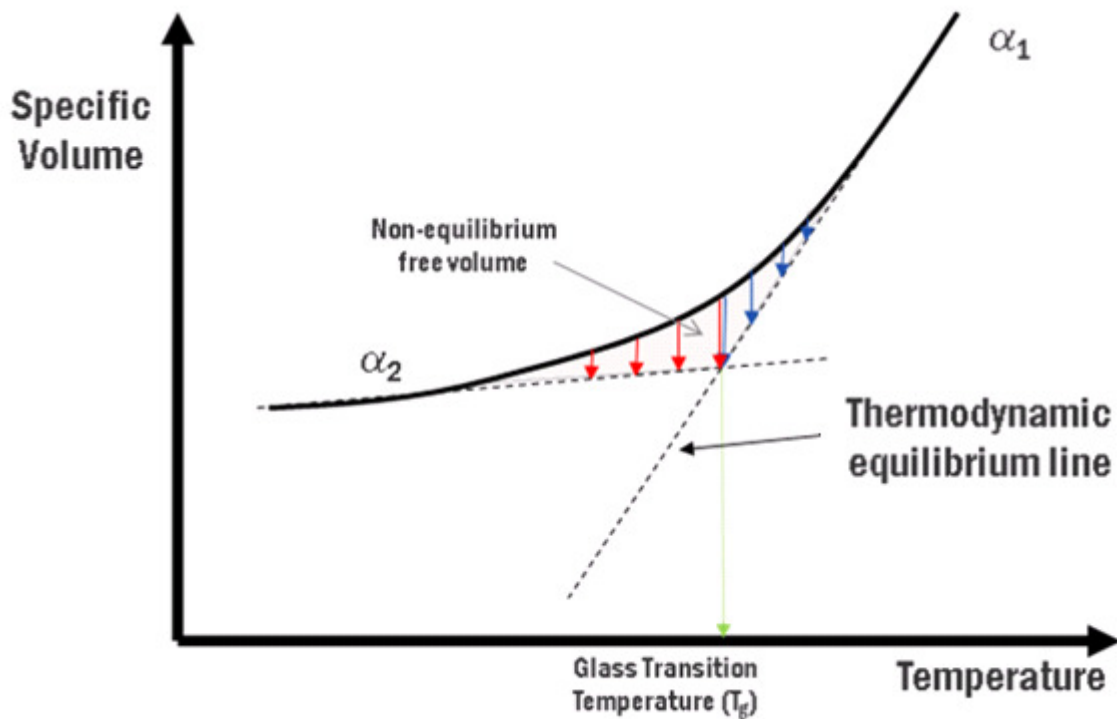
Figure 7: Schematic of proposed material behavior in glass transition region.

Effect of Thermal History

The asphalt binders described in Table 2 were used to investigate the influence of thermal history on the development of physical hardening. Figure 8 shows typical results of the effect of thermal history on the creep stiffness (S) of binders. The thermal cycle applied to the PG 58-34 +PPA binder from MnROAD 33 is depicted as the solid blue line in Figure 8.

Although absolute values represent an indication of how stiffness and m-value (i.e., relaxation property) change during the thermal cycle, a better indication of the development of physical hardening is obtained when relative changes are used. Therefore, both properties, stiffness and m-value at 60 seconds, were normalized with respect to their value at the beginning of each isothermal period (i.e., S(60) and m(60) at 1 hour of conditioning). Figure 9 shows the normalized values for creep stiffness (S) and m-value at 60 seconds during the thermal cycle for all binders.

Figure 8: PG 58-34+ PPA binder from MnROAD 33- creep stiffness as function of conditioning time.

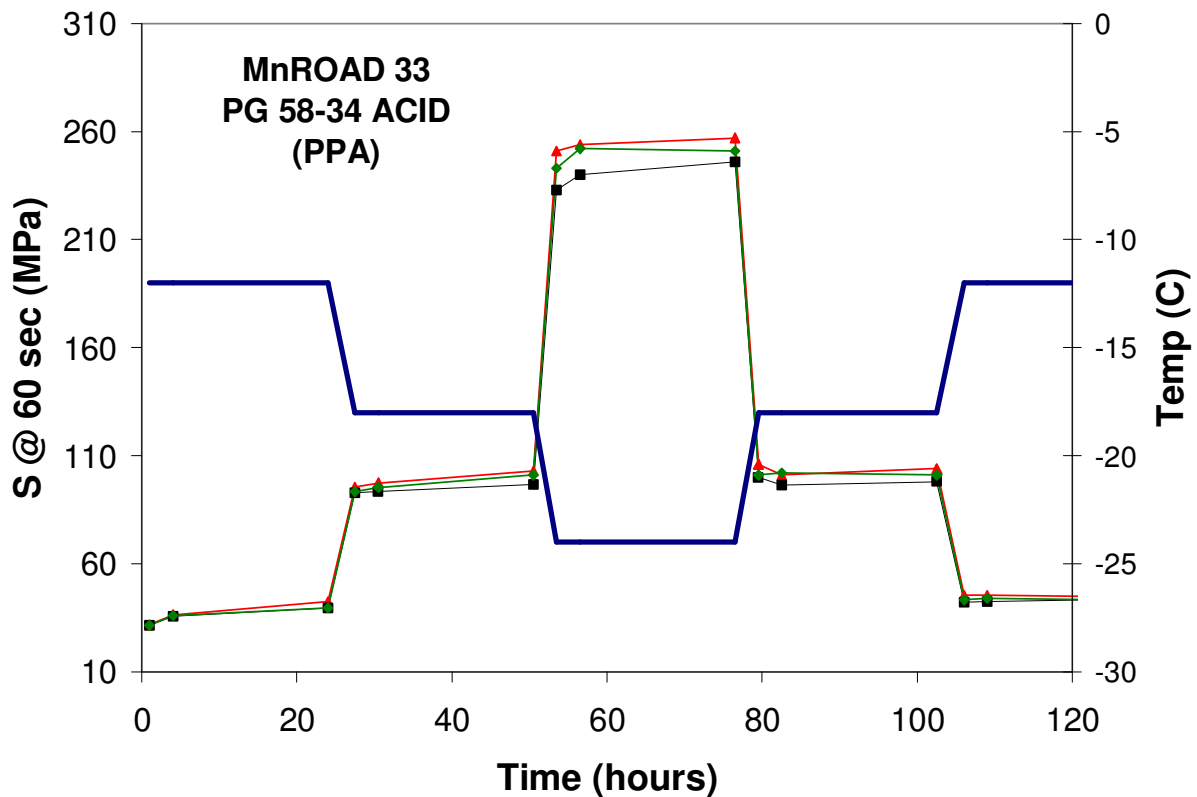Figure 9 indicates that significant physical hardening was observed during the first conditioning period after reducing the temperature from 25°C (i.e., room temperature) to -12°C. During the subsequent conditioning periods (i.e. further cooling), the asphalt binders showed a significant reduction on the magnitude and rate of hardening, confirming the influence of previous conditioning periods or thermal history on physical hardening. During the heating component of the thermal cycle, mechanical properties of the asphalt binders remained approximately unchanged regardless of the isothermal conditioning time. During the heating phase of the thermal cycle, the asphalt binder is very close to the thermodynamic equilibrium line. Therefore, when heated from a lower to a higher temperature, the amount of free volume available for isothermal contraction is minimal and thus any molecular adjustment will be extremely slow. Then, as it can be seen in Figure 9, no physical hardening is observed in terms of stiffness and m-value within the experimental time of the isothermal conditioning periods at -18°C and -12°C in the heating phase. Note that New York binder was not available to the research team when performing these tests.
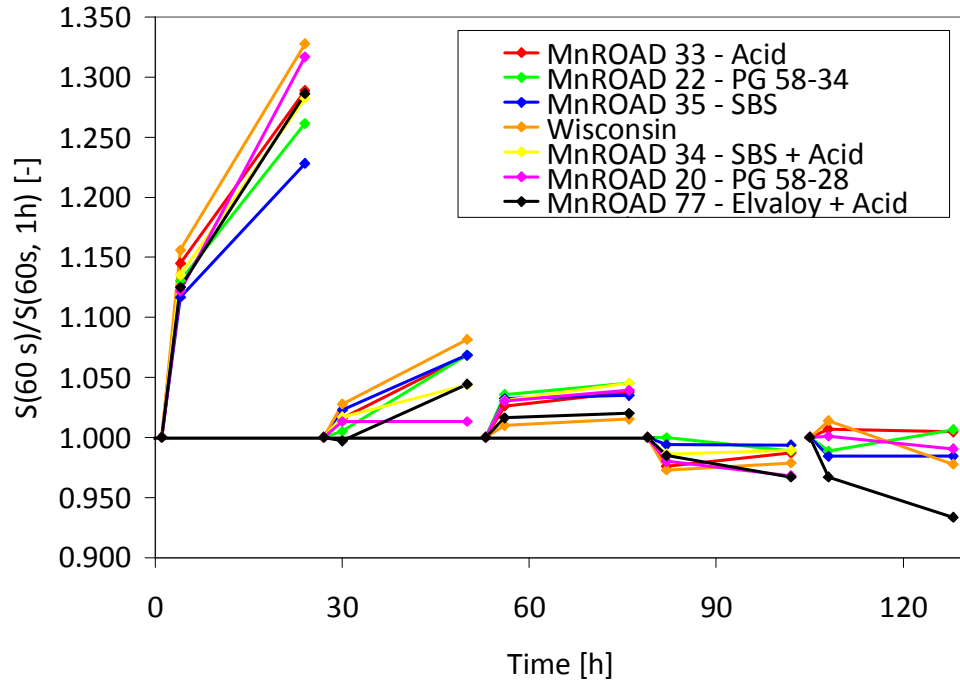
(a)
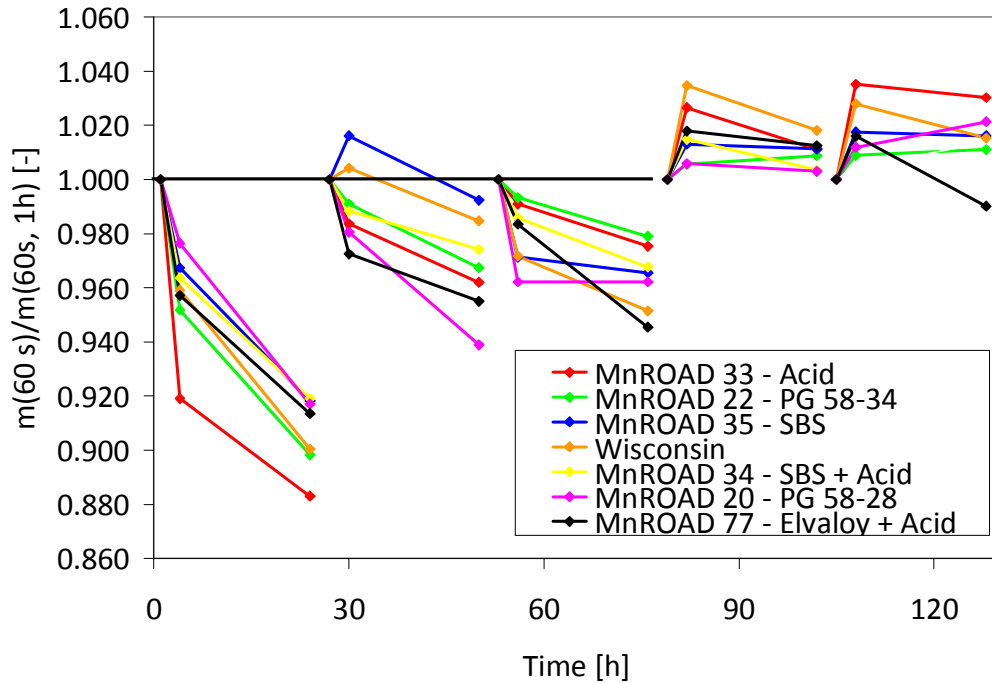
(b)

Figure 9: Effect of thermal history on physical hardening by measuring changes in creep stiffness and m-values of binders in Table 2.

Further evidence of this effect can be found by observing the creep curves from the single BBR tests performed during the thermal cycle. The creep curves for different conditioning times

are well distinguishable during the isothermal period immediately following the initial quench at -12 °C. However, they become closer and closer for the two isothermal periods at -18 °C and -24 °C, proving that physical hardening occurrence is reduced. Finally, during the isothermal periods in the heating ramp, creep curves are practically superimposed on each other, revealing the absence of remarkable physical hardening within the experimental time scale.

Development of Model to Predict Physical Hardening

The proposed model is built upon concepts of rheological response of viscoelastic materials. In rheology creep is defined as the progressive deformation under a constant stress. Creep in a linear material is a function of time only (21). One may describe creep as the gradual redistribution of the molecules, resulting in a change in free volume and a decrease in the creep stiffness (increase in creep compliance). Similarly in hydrostatic (volumetric) stress conditions this phenomenon can be observed, where under a fixed stress level, free volume gradually decreases over time, causing a gradual increase in stiffness. The Burger's model is often used to model the creep behavior in asphalt:

$$\gamma = \frac{\tau}{G_0} + \frac{\tau}{G_1}\left(1 - e^{-t\frac{G_1}{\eta_1}}\right) + \frac{\tau}{\eta_0}t \qquad [1]$$

where, γ is the strain resulting from the creep, τ is the applied stress, t is loading time and G_0, G_1, η_0 and η_1 are the elastic and viscous material constants. Burger's model consists of a Maxwell and Kelvin models in series. At lower temperatures the effect of physical hardening can be described by the Kelvin model as there is no significant instatntanuous change in volume after thermal equilibrium is chaoeve.

$$\gamma = \frac{\tau}{G_1}\left(1 - e^{-t\frac{G_1}{\eta_1}}\right) \qquad [2]$$

The creep behavior at the molecular level could be envisioned as similar to the behavior observed in physical hardening. The basic property that changes during physical hardening is segmental or molecular mobility; which is also claimed to be directly related to deformation under creep loading (6). The amount of free volume controls molecular mobility, which in turn controls the rate of volume change which is responsible for the rate of hardening. Thus, the controlling factor in the hardening rate would be the volume difference relative to the equilibrium state, as shown in Figure 7. This difference increases as temperature approaches the glass transition temperature in Figure 7, after which it starts to decrease. This concept explains the mechanism behind the observed trend in hardening rate as temperature decreases.

Thus, it is hypothesized that a modified creep model can be adjusted to fit physical hardening behavior. In such a model, strain or relative change in deflection (i.e., $\Delta l/l_0$), can be replaced by relative change in volume, $\Delta V/V_0$, which according to the free volume concept can be taken to be directly proportional to relative change in stiffness, or hardening rate ($\Delta S/S_0$). Hardening rate can be measured in the laboratory with the BBR and thus used as input in the model in place of $\Delta V/V_0$. The change in stiffness (ΔS) is calculated as the difference in S(60) at time t_i and at time t_0, which is the S(60) at one hour conditioning.

Creep is usually driven by the stress of an applied load. In the physical hardening case, the "creep" behavior at isothermal conditions was considered to be induced by the excess

internal energy due to the deviation of the material from thermo-dynamic equilibrium within the glass transition region, thus a "stress" parameter based on the glass transition temperature, relative position of the conditioning temperature from the glass transition temperature and the length of the glass transition region was envisioned for the model. In this case the loading time would be the length of time the material is in temperature at which the material is not at thermo-dynamic equilibrium, or in other words, the conditioning time (t_c).

As described previously, the rate of physical hardening (, peaks at a certain temperature, hereby denoted as T_0, and decreases toward zero as the temperature approaches the beginning and the end of the glass transition region, as is shown in Figure 10. This trend was taken into account to formulate the "stress" term for the model. For the current study, the following empirical equation was shown to fit the observed behavior of physical hardening very well:

$$\overline{}$$

[3]

In this equation τ_T is the "stress" term as a function of the temperature at which physical hardening peaks, T_0, and the length of the glass transition region, $2x$.
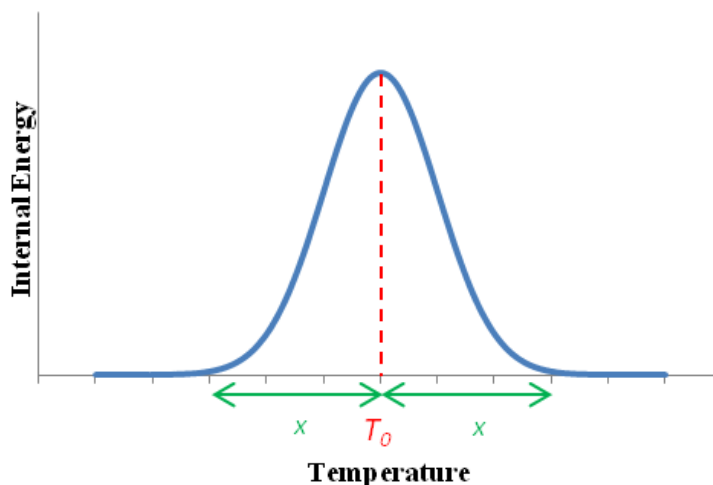
Figure 10: Empirical function used to account for glass transition temperature in prediction model. ($2x$ is the length of the glass transition region)

From the experimental data it was recognized that the Internal energy variation around temperature T_0 is not completely symmetrical, but is in fact slightly skewed toward the lower temperatures, but for simplicity a symmetric formulation was used in [3]. Using [2] and [3], the model is rewritten as:

$$\overline{} \qquad \overline{}$$

$$\overline{}\ \overline{}\ \overline{}$$

[4]

In which:

- — is the change in hardening relative to the hardening after 1 hr of conditioning.
- T_0 is the peak temperature for hardening rate, assumed to be the T_g (°C)
- T is the conditioning temperature (°C)

- t_c is the conditioning time (hrs)
- *2x* is the length of the temperature range of the glass transition region (°C)
- *G* and *η* are model constants, derived by fitting the model

This model was fitted to the experimental data using the least sum of squared errors method, replacing T_0 with the glass transition temperatures measured using the dilatometric method as reported by Bahia (2) and allowing the model to fit the length of the glass transition region to the data. As shown in Figures 11 and 12, the results accurately predict the experimental data. The model predicted the observed data for all test temperatures. Furthermore, the model predicted a decrease in hardening rate as the temperature passed the glass transition temperature, as was evident in the experimental data from the samples conditioned at -35°C. A goodness of fit of 92% observed between measured and predicted hardening rates for the 8-core SHRP binders indicates the validity of assuming the glass transition temperature to be the peak temperature for the rate of physical hardening (Figure 12).

In a second set of runs instead of inputting the glass transition temperature as the peak temperature, the model was allowed to find the peak temperature based on the best fit to the experimental data. The resulting fitted peak temperatures were only within a few degrees of the measured glass transition temperatures. This indicates that if data from a few temperatures is available, the model can be used to estimate the T_g from the experimental hardening rate data. Figure 13 shows the goodness of fit of the model for fitted values.
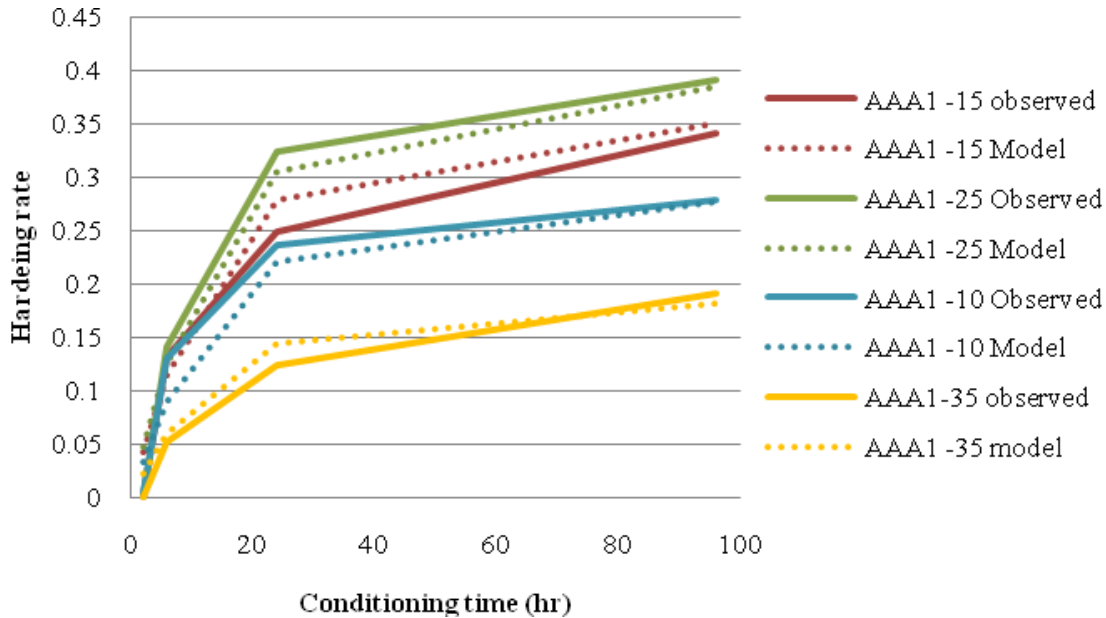

Figure 11: Comparison of model described by [4] with experimental data. (Hardening rate= ΔS/S$_0$)
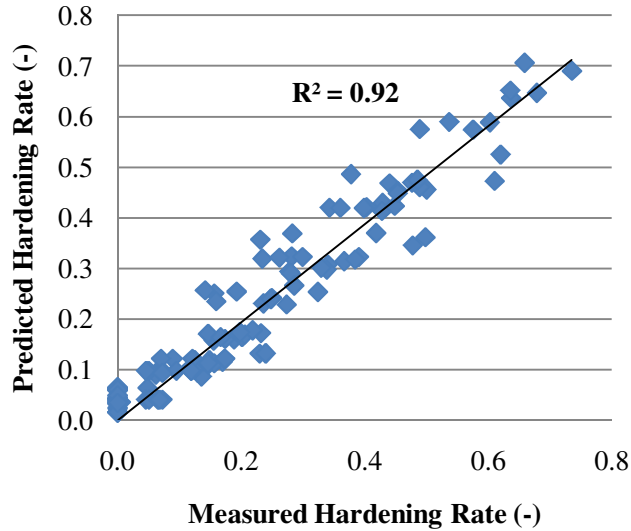
Figure 12: Goodness of fit between the predictions using Equation [4] using T_g for T_0 and the experimental data. (Hardening rate= $\Delta S/S_0$)
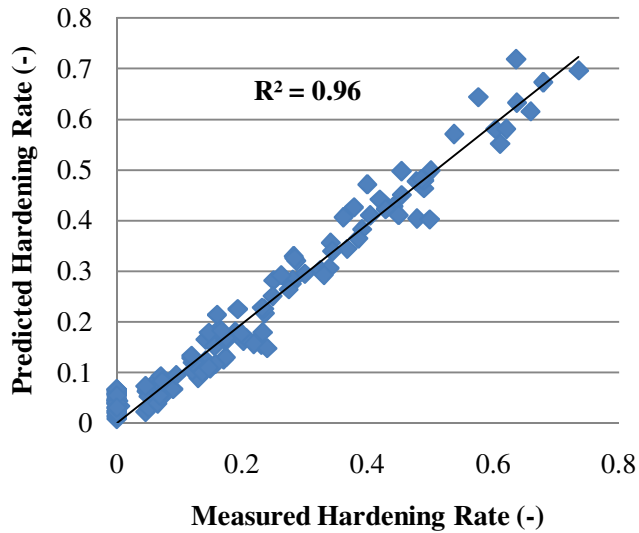
Figure 13: Goodness of fit between model described by [4] with fitted T_0 and experimental data. (Hardening rate= $\Delta S/S_0$)

It must be noted that for every binder, G and η are unique material parameters which are independent of temperature and conditioning time. Thus, by fitting the model to data from a single temperature, one may use the resulting G and η to predict the physical hardening at any other temperature or conditioning time.

The most important objective of developing this model is the ability to enable prediction with fewer tests or easily available data. For the proposed model, two possible prediction methods are considered. The first and simplest method would be to use 3 hardening rate data

points from a BBR test carried out at a single temperature after relatively short conditioning times along with the glass transition temperature to fit the model and use the resulting G and η to predict the effect of much longer conditioning times or other conditioning temperatures. Although this is an improvement compared to the much longer conditioning times as well as other temperatures. It must be noted that as with any non-linear model, the closer the input data points are to each other (or in this case, the shorter the conditioning times used), the lower the accuracy of the extrapolation of the model to much longer conditioning times.

The second method is to find regression functions that can be used to relate BBR creep stiffness S(60) or m-value at 1 hour conditioning, to predict the model parameters G and η. A promising relationship was observed between S(60) and conditioning temperature from the SHRP binders and the model parameters. As shown in Figure 14, a power law was fitted to the curve for all binders and the A and B parameters were determined as described in [5].

$$S(60) = A|T|^B \hspace{4cm} [5]$$

Figure with y-axis "S(60) (MPa)" and x-axis "Test Temperature (Absolute value in terms of °C)"; fitted equation $y = 0.01x^{3.25}$, $R^2 = 0.99$.
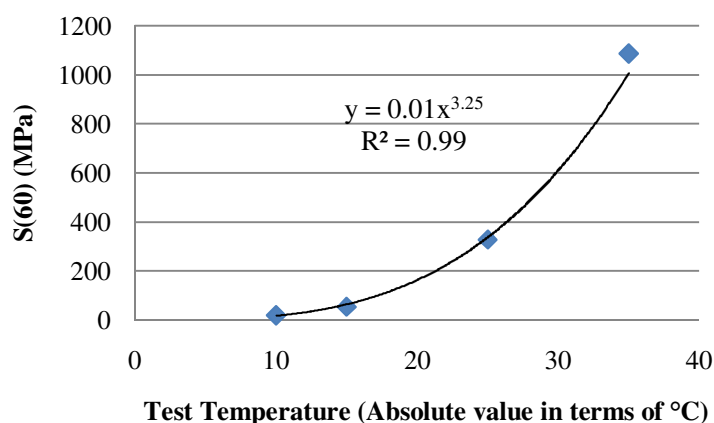
Figure 14: S(60) after 1 hr conditioning for one of the SHRP binders plotted against test temperature.

The A and B parameters were plotted against G and η. No apparent relationship existed with the A parameter. However, an interesting correlation was established using B from the SHRP binders. The relationships can be seen in Figure 15.
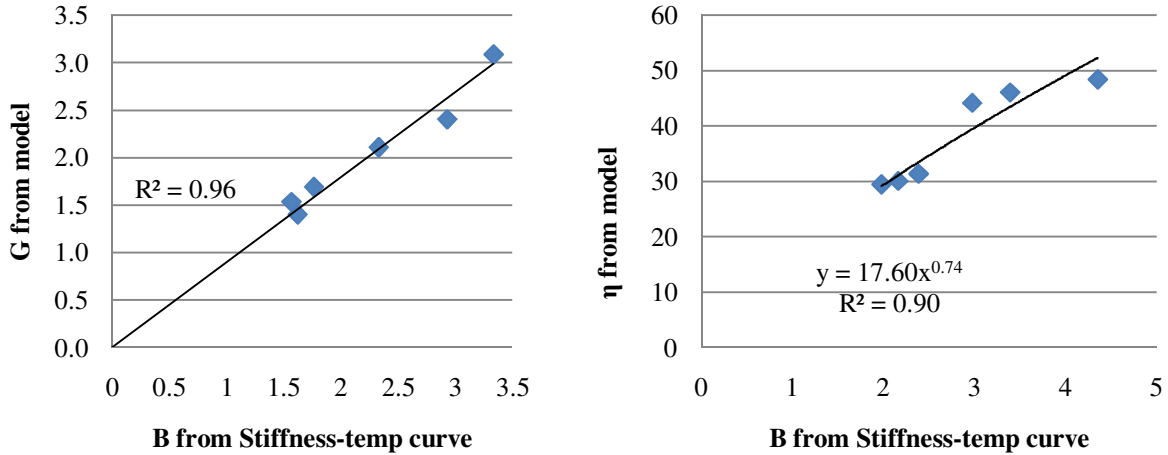
Figure 15: Correlation between *G* and *η* and *B* for the SHRP binders.

The correlations showed that parameter *G* and parameter *B* are in equality. This equality is very intriguing and more investigation into this relationship may be warranted. Using the relationships shown in Figure 15, [4] can be rewritten as:

$$\frac{\Delta S}{S_0} = \frac{e^{\frac{-9(T-T_0)^2}{(2x)^2}}}{B}\left(1 - e^{\frac{-t_c B^{0.26}}{17.6}}\right) \qquad [6]$$

In which:

- $\frac{\Delta S}{S_0}$ is the change in hardening relative to the hardening after 1 hr of conditioning.
- T_0 is the peak temperature for hardening rate, assumed to be the T_g (°C)
- T is conditioning temperature (°C)
- t_c is the conditioning time (hrs)
- $2x$ is the length of the temperature range of the glass transition region (°C)
- B is derived from [5]

Equations such as [6] can be used to predict the hardening rate for other binders at any temperature and conditioning time, using only S(60) at 1 hr from BBR grading tests and the T_g. A comparison between this predicted model and the measured data is presented in Figure 16 for the tested binders. The applicability of using the proposed physical hardening model for different binders will increase as data from more binders are used to refine the observed relationship between the parameters. Although requiring measuring T_g may be inconvenient, this study has clearly shown that the glass transition behavior of a binder is one of the controlling factors in the physical hardening phenomenon and no model can accurately describe it without taking the glass transition into account.
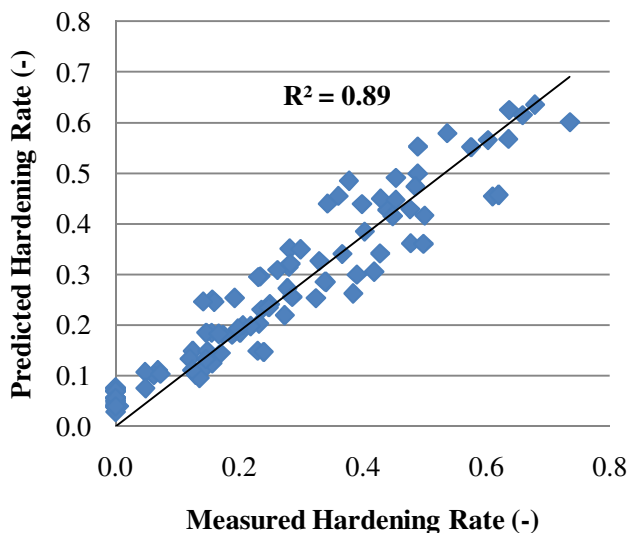
Figure 16: Goodness of fit between model described by [6] using T_g for T_0 and experimental data.

Physical Hardening in MnROAD Binders

The asphalt binders described in Table 2 comprised of four neat binders (MnROAD 20, 22, New York and Wisconsin) and four modified binders with the same base (MnROAD 33, 34, 35 and 77). The proposed physical hardening model was fit to experimental data from these binders by both inputting the dilatometric measurement of the glass transition temperature and by allowing the model to fit the model to the best glass transition temperature. As it can be seen in Figure 17, in both cases the goodness of fit was very good and the measured and predicted glass transition temperatures were within a few degrees of each other. Figures 20-22 compare the G, η and average hardening for all 8 binders.

(a)

(b)
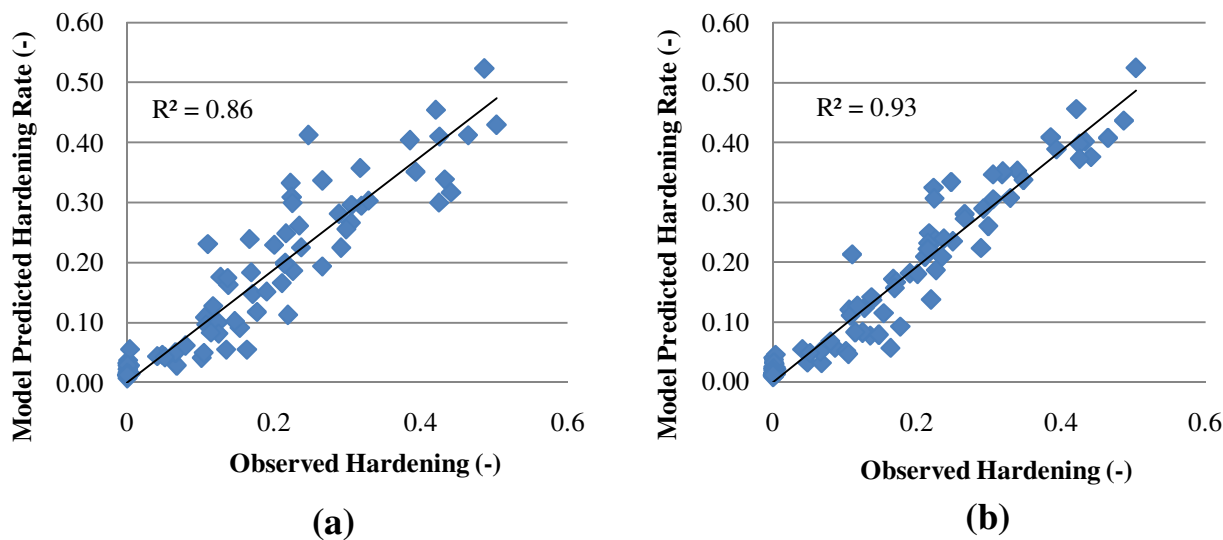
Figure 17: Goodness of fit of the physical hardening model for the MnROAD binders (a) using measured glass transition temperature values, (b) using values fitted by model.
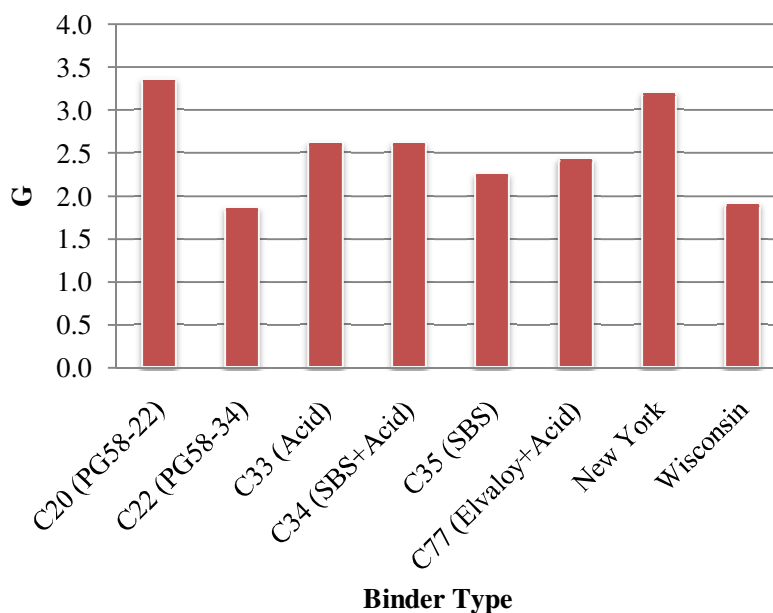
Figure 18: Comparison of the *G* parameter derived from the fitted physical hardening model.
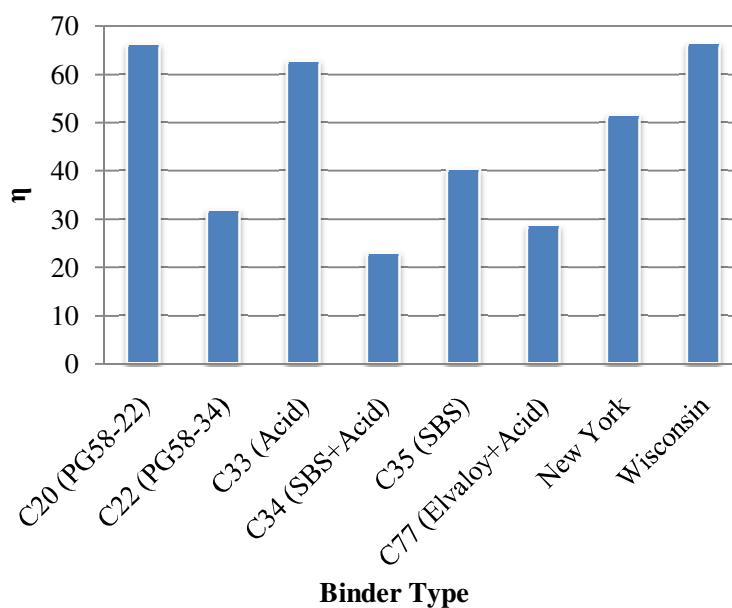
Figure 19: Comparison of the η parameter derived from the fitted physical hardening model.

Ranking of the *G* parameter shows that MnROAD cell 22 and the Wisconsin binder are the most prone to physical hardening, while MnROAD cell 20 and New York binder are the least susceptible to hardening among the eight tested binders. Note that this is also reflected by the estimated average hardening obtained from the BBR tests as indicated in Figure 20.

It was observed that the polymer modified binders, MnROAD cells 34, 35, and 77, have very similar physical hardening susceptibility. This indicates that although the type of polymer modifier has changed, the amount of physical hardening remains almost constant. This trend was noted earlier through the review of existing test data from other studies. It was concluded that due to the predominant effect of the base binder phase in the two-phase polymer modified binder system, the polymer phase does not significantly alter the physical hardening behavior of the binder and thus polymer type becomes insignificant compared to the base binder type.
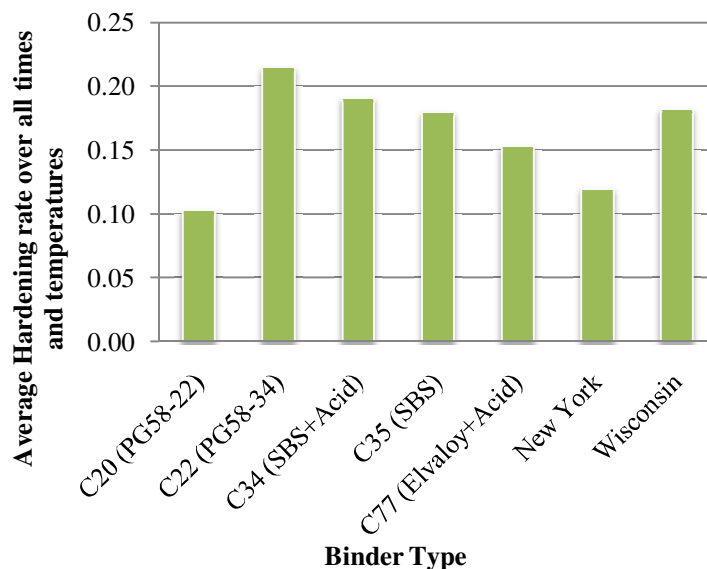

Figure 20: Comparison of the average hardening for each binder over all tested conditioning times and temperatures.

Effect of Polyphosphoric Acid (PPA) and Warm Mix Additives (WMA)

The effect of Polyphosphoric Acid (PPA) and a Warm Mix Additive (WMA) on physical hardening was investigated by performing tests on a PG 64-22 binder modified with PPA and Sasobit (i.e., a wax commonly used as a warm mix additive in the pavement industry).

BBR beams were prepared for each binder and kept for isothermal conditioning at -12, -18 and -24°C for 72 hrs. The creep stiffness and m-value were measured after 1, 4, 24, and 72 hrs of conditioning. The proposed physical hardening model was fitted to the test results. As glass transition measurements were not done for these binders, the model was allowed to predict the glass transition temperature. It was noted that the predicted T_g decreased when PPA was added to the binder, but increased when Sasobit was added. This result indicates that binders containing Sasobit become brittle sooner than the binders modified with PPA. Consequently an inferior thermal cracking resistance will be expected in comparison to the neat and PPA modified binder.

The average hardening rate over all tested temperatures and conditioning times are shown in Figure 21. Figures 22 and 23 present a comparison of the model parameters for the tested binders. It can be seen that the binder containing PPA has a relatively smaller G, thus showing a higher hardening potential. The η parameter for the PPA modified binder is also lower, meaning that the hardening, although comparatively larger in magnitude, builds up at a relatively slower rate compared to the binder with Sasobit or the base binder. It was observed that the Sasobit

decreased the magnitude of hardening; however it increased the rate at which this phenomenon develops. These trends are supported by the average hardening parameter presented in Figure 21. These experimental results indicate that PPA and WMA do indeed have a significant effect on the physical hardening of asphalt binders.
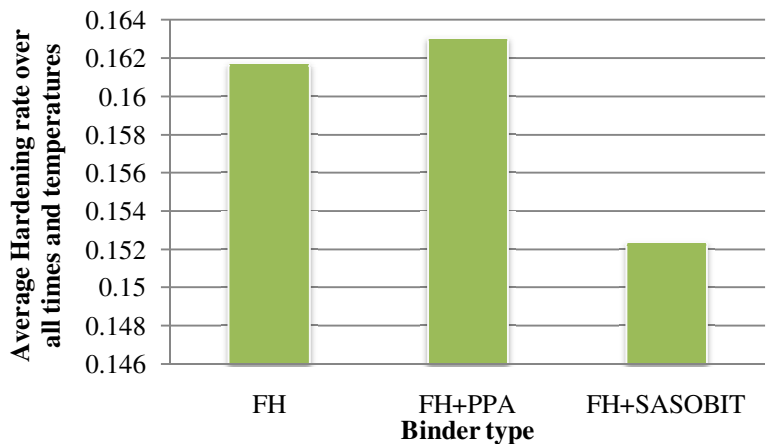

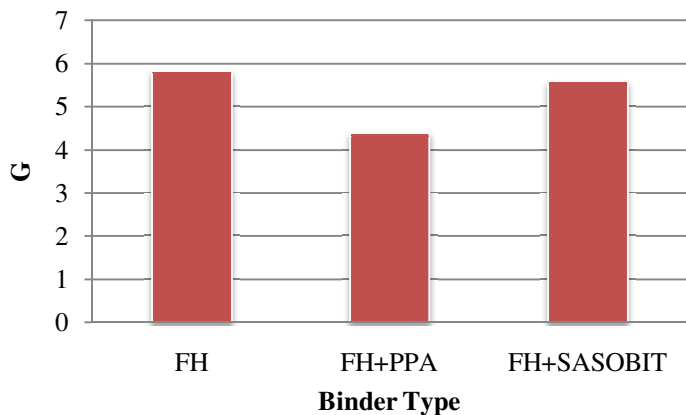**Figure 21: Comparison of the average hardening for each binder over all tested conditioning times and temperatures.**

Figure 22: Comparison of *G* parameter derived from the fitted physical hardening model.
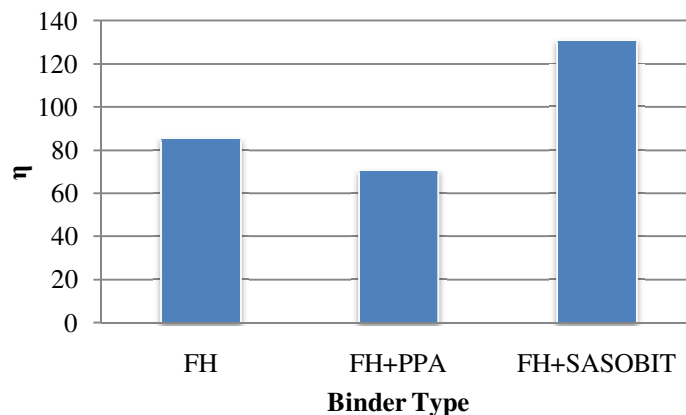
Figure 23: Comparison of the η parameter derived from the fitted physical hardening model.

Dimensional Stability of Asphalt Mixtures During Isothermal Storage

The glass transition procedure for asphalt mixtures was modified to quantify effect of isothermal storage on dimensional stability of asphalt mixtures. Previously, glass transition measurements for asphalt mixtures were conducted using beam samples cut from slab compacted mixtures. However, since slab compactors are not readily available in many agencies and laboratories, the usefulness of a test requiring such machinery would be limited. Therefore, the new testing procedure focused on developing an adequate T_g sample geometry that is relatively easier to produce and prepare using equipment accessible in most laboratories.

Three possible preparation procedures, which use gyratory compacted samples, were investigated before selecting the optimal solution. The first two methods were based on coring the samples and gluing the cores which were 1" and 2.5" in diameter, respectively. The final specimen after gluing was approximately 12" long. This minimal length is required in glass transition temperature measurements of mixtures to allow measurable changes in length of the sample. Taking into account the usual height of a gyratory compacted sample, three cores are required for such a sample.

The first step was to confirm that the glue in the samples did not affect the glass transition measurements. Figure 24 shows the results for glass transition temperature obtained from a mixture sample tested before and after cutting to 3 pieces and gluing back together using an epoxy resin. The results indicate that the glass transition behavior is unaffected by the gluing procedure.
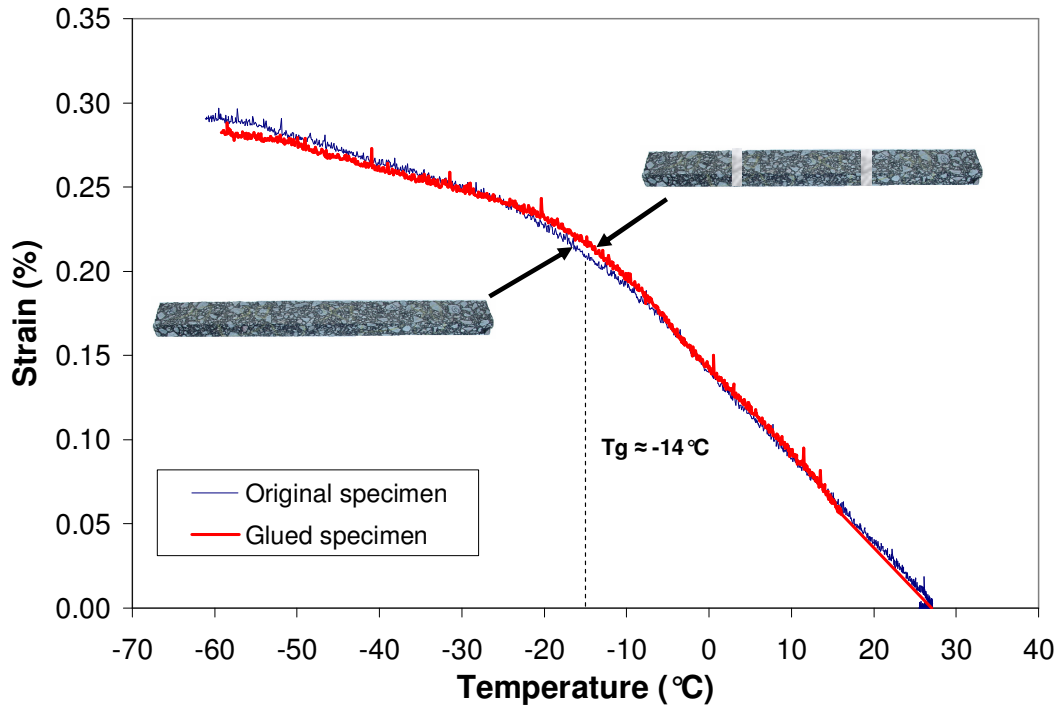
Figure 24: T$_g$ mixture results for unglued and glued specimen.

Then, glass transition tests were run on the samples with different diameters and the results showed that the core diameter did not significantly affect the glass transition measurements. It is observed in Figure 25 that both specimen sizes yielded similar glass transition temperatures. The main issue of the 2.5" specimen is the difficulty in extracting more than one core from each gyratory compacted sample. Furthermore, for the 1" specimen, concerns about size effects (e.g., specimen smaller than the representative volume element, RVE) prevented the research team to move forward with these geometries. Consequently, a third method which involves a prismatic geometry was considered. In the third method instead of coring, a few cuts were made in the gyratory compacted sample using a masonry saw, such that four prismatic beams of about 2 x 2" in cross section and about 4" long were produced. Three of these beams were glued to each other using epoxy resin to produce a 12" long prismatic beam (Figure 25). It was observed that this method was less time consuming than the coring methods and that the samples were easier to glue. Furthermore, positioning the sample on the rollers and between the two LVDTs was much easier as the sample geometry prevented it from moving laterally as it was in the case of the cylindrical samples produced from coring.
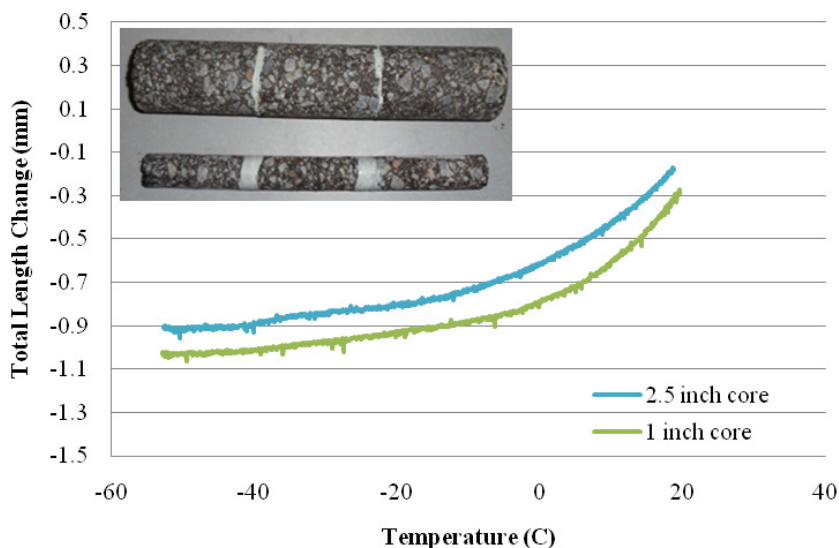
Figure 25: Comparison of T$_g$ results from samples with φ =1" and 2.5".

Figure 26: Prismatic beams made from gluing blocks cut out of gyratory samples.

Figure 27 shows the final setup used for the glass transition tests of asphalt mixtures. The LVDTs used in the T$_g$ device were tested for linearity and accuracy using a micrometer. Furthermore, the setup was also checked by testing a Nickel rod with known coefficient of thermal contraction/expansion. The results of tests with cooling and heating cycles confirmed that the setup is not introducing any bias in the results.

Figure 27: Test setup used for the glass transition temperature of beams made from gyratory compacted samples

Preliminary tests to investigate the effect of isothermal storage on the dimensional stability of asphalt mixtures were conducted. The volumetric stability at isothermal conditions was tested with the T_g setup by decreasing the temperature to -25°C and then holding the temperature constant for conditioning. A decreasing length over time is visible over the course of the isothermal conditioning. The isothermal reduction in length of the asphalt mixture measured after only 200 minutes (3.3 hours) was of a magnitude of about 7% of the total length change when the temperature is reduced from 30 to -25°C. Two independent replicates showed the same phenomenon. Further tests for longer times and more analysis of results are required to investigate the exact nature of the dimensional stability of asphalt mixtures due to isothermal storage.

Summary of Findings and Conclusions

Although researchers have been aware of physical hardening as a factor influencing low temperature properties of binders, the factors that affect this phenomenon are not well defined. The purpose of this task was to understand how physical hardening is affected by parameters such as temperature, conditioning time, modification, thermal history, and glass transition temperature, and to propose a comprehensive model in which the physical hardening of asphalt binders can be predicted for different conditions without lengthy tests. The tests performed in this study were combined with experimental data from previous studies to enable a broad analysis of the nature of physical hardening in asphalt binders and to propose a model. Based on the results, the following important conclusions were made:

- Physical hardening in asphalt binders results in significant changes in their creep response at temperatures below or near the glass transition. This phenomenon can be successfully characterized by a horizontal shift of the creep response along the loading time scale. The horizontal shifting indicates that the influence of physical hardening is similar to the influence of lowering temperature in thermo-rheological simple materials.

- The rate of physical hardening decreases rapidly with isothermal age and it is highly dependent on conditioning temperature and the source of the base binder. Different types of polymer modification did not significantly change the rate of physical hardening. This was explained as being the result of the two-phase nature of polymer modified binders, in which the hardening behavior of the base binder phase is dominant.

- The rate of physical hardening does not increase indefinitely as temperature decreases. Based on literature review and the experimental data collected, it is hypothesized that the rate of hardening peaks at a specific temperature, and approaches zero as the temperature increases or decrease toward the limits of the glass transition region. It was shown that the peak temperature corresponds to the glass transition temperature of the binder.

- The rate and magnitude of physical hardening is highly dependent on the thermal history applied to the asphalt binder. Creep tests performed over the course of a thermal cycle consisting of five consecutive isothermal conditioning periods of 26 hours at three different temperatures indicate that physical hardening occurs mostly during the first isothermal period. Both, the magnitude and rate of hardening is significantly reduced for the rest of the isothermal periods in the cooling phase. Moreover, insignificant hardening is observed during the isothermal periods in the heating phase of the thermal cycle. This

results show the non-symmetric behavior of physical hardening during cooling and heating cycles.

- A modified creep model was shown to be able to reflect the change in physical hardening rate with conditioning time and temperature. The model parameters, G and η, were shown to be unique material parameters that remain constant at all conditioning times and temperatures. Thus, by fitting the model to three stiffness values at a single temperature, and by having the $T_{g\ value}$, one may predict the physical hardening at any other temperature or conditioning time. The developed model can also be used to estimate T_g using physical hardening test results from 3 or more temperatures.

- The model was rewritten using correlations from existing PG grading data, making it possible to predict the hardening for any binder at any temperature and conditioning time using $S(60)$ at 1 hr from BBR tests at multiple temperatures, the binder T_g, and the width of the glass transition region. Future work should focus on refining this relationship by increasing the pool of experimental data and binders used for developing the regression equations.

References

1. Anderson, D., Christensen, D., Bahia, H.U., Dongre, R., Sharma, M., Antle, C., and Button J. "Binder Characterization and Evaluation Vol. 3: Physical Characterization. SHRPA-369", Strategic Highway Research Program, National Research Council, Washington, D.C. (1994).

2. Bahia H.U., Low-Temperature Isothermal Physical Hardening of Asphalt Cements. Ph.D. Thesis. Pennsylvania State University, (1991).

3. American Association of State Highway and Transportation Officials (AASHTO) M320, "Standard Specification for Performance-Graded Asphalt Binder", AASHTO Provisional Standards, Washington, D.C. (2002).

4. Hesp, SAM and Subramani, S. "Another Look at the Bending Beam Rheometer for Specification Grading of Asphalt Cements", Proceedings of 6th MAIREPAV Conference, Torino, Italy, (2009).

5. Lu, X., and Isacsson, U., Laboratory Study on the Low Temperature Physical Hardening of Conventional and Polymer Modified Bitumens, Construction and Building Materials, Vol. 14, pp. 79-88, (2000).

6. Struik, LCE., Physical Hardening in Amorphous Polymers and Other Materials, Elsevier, (1978).

7. Ferry, J.D., Viscoelastic Properties of Polymers, 3rd Edition, Wiley, New York, NY, (1980).

8. Doolittle, A.K., "Studies in Newtonian Flow. II The Dependence of Viscosity of Liquids on Free-Space", Journal of Applied Physics 22 (12), pp. 1471, (1951).

9. Doolittle, A.K., and Doolittle, D.B., "Studies in Newtonian Flow. V Further Verification of the Free Space Viscosity Equation", Journal of Applied Physics 28 (8), pp. 901, (1957).

10. Williams, M.L., Landel, R.F., Ferry, J.D., "The Temperature Dependence of Relaxation Mechanisms in Amorphous Polymers and Other Glass-forming Liquids", Journal of the American Chemical Society 77, pp. 3701-3706, (1955).

11. Brandrup, J., Immergut, E.H., Grulke, E.A., Polymer Handbook, 4th Edition, Wiley-Interscience, New York, NY, (2003).

12. Claudy, P., Planche, J.P., King, G., Letoffe, J.M., "Characterization of Asphalt Cements by Thermomicroscopy and Differential Scanning Calorimetry: Correlation to Classic Physical Properties", Proceedings of the 204th American Chemical Society National Meeting, Division of Fuel Chemistry 37 (3), (1992).

13. Kriz, P., Stastna, J., Zanzotto, L., "Physical Aging in Semi-Crystalline Asphalt Binders", Journal of the Association of Asphalt Paving Technologists 77 pp.795-825, (2008).

14. Anderson, D.A., and Marasteanu, M.O., "Physical Hardening of Asphalt Binders Relative to Their Glass Transition Temperatures", Transportation Research Record: Journal of the Transportation Research Board 1661 pp. 27-34, (1999).

15. Marasteanu, M.O., Low-Temperature Inter-Conversions of the Linear Viscoelastic Functions for the Rheological Characterization of Asphalt Binders. Ph.D. Thesis. Pennsylvania State University, (1999).

16. Romero, P., Youtcheff, J., Stuart, K., "Low-Temperature Physical Hardening of Hot-Mix Asphalt", Transportation Research Record: Journal of the Transportation Research Board 1661 pp. 22-26, (1999).

17. American Association of State Highway and Transportation Officials (AASHTO) Standard T313-05, "Standard method of test for determining the flexural creep stiffness of asphalt binder using the Bending Beam Rheometer (BBR)", Standard Specifications for Transportation Materials and Methods of Sampling and Testing, 25th Edition, (2005).

18. Bahia, H. and Anderson, D., "Glass Transition Behavior and Physical Hardening of Asphalt Binders," Journal of the Association of Asphalt Paving Technologists, Vol. 62, pp. 93-129, (1993).

19. Nam, K. and Bahia, H., "Effect of Binder and Mixture Variables on Glass Transition Behavior of Asphalt Mixtures", Journal of the Association of Asphalt Paving Technologists, Vol. 73, pp. 89, (2004).

20. Johansson, L. and Isacsson, U., Effect of filler on low temperature physical hardening of bitumen, Construction and Building Materials, Vol. 12, pp. 463-470, (1998).

21. Lakes, R., Viscoelastic Materials, Cambridge University Press, New York, (2009).